NJC

Accepted Manuscript

This is an *Accepted Manuscript*, which has been through the Royal Society of Chemistry peer review process and has been accepted for publication.

Accepted Manuscripts are published online shortly after acceptance, before technical editing, formatting and proof reading. Using this free service, authors can make their results available to the community, in citable form, before we publish the edited article. We will replace this *Accepted Manuscript* with the edited and formatted *Advance Article* as soon as it is available.

You can find more information about *Accepted Manuscripts* in the Information for Authors.

Please note that technical editing may introduce minor changes to the text and/or graphics, which may alter content. The journal's standard Terms & Conditions and the Ethical guidelines still apply. In no event shall the Royal Society of Chemistry be held responsible for any errors or omissions in this *Accepted Manuscript* or any consequences arising from the use of any information it contains.

ROYAL SOCIETY OF CHEMISTRY

www.rsc.org/njc

Microwave-assisted green synthesis of some nanoconjugated copolymers: Characterisation and fluorescence quenching studies with bovine serum albumin

Ufana Riaz*, S.M.Ashraf[+], Sadaf Aleem, Vaibhav Buddhiraja and Sapana Jadoun

Materials Research Laboratory, Department of Chemistry Jamia Millia Islamia (A Central University), New Delhi-110025, India *Corresponding author: Fax-(+91-112-684-0229); E-mail address-(ufana2002@yahoo.co.in), [+] Now retired

Abstract

Copolymerization is an effective technique to design conjugated polymers with properties higher than individual homopolymers, as the composition and the desired chemical properties can be controlled by the judicious choice of co-monomers and polymerization technique. With a view to explore the influence of microwave-assisted copolymerization on the spectral and fluorescent properties of some functionalized monomers, the present work reports for the first time, synthesis of conjugated copolymers of poly(1-naphthylamine), poly(o-phenylenediamine), poly(o-anisidine) under microwave irradiation. Fourier transform infrared spectroscopy confirmed random copolymerization while ultra violet-visible studies revealed the variation in the polaronic states upon copolymerization. High crystallinity was achieved through the formation of distorted orthrhombic lattice and controlled morphology via microwave-assisted synthesis which was confirmed by X-ray diffraction and transmission electron microscopic analysis. This behaviour was explained on the basis of variable orientations adopted by the conducting polymer chains. A water soluble homopolymer and a copolymer were tested for the deactivation of bovine serum albumin's fluorescence and the former was found to effectively quench the fluorescence emission of the later. Quenching occured through formation of intermolecular complex and was initiated by photo induced electron transfer and was observed to be static in nature. Quenching rate constant, k_q, for POPD and POPD-co-PNA was found to be 1.08 x10^{14} LM^{-1} s^{-1} and 2.0x10^{14} L M^{-1} s^{-1} revealing much higher quenching rate constant k_q for the copolymer than homopolymer. Likewise, binding constant, K_a, for homopolymer and copolymer were observed to be 3.98 x 10^6 $Lmol^{-1}$ and 1.26 x 10^7 $Lmol^{-1}$ revealing much higher binding constant for copolymer POPD-co-PNA than homopolymer POPD. Confocal microscopy revealed widely distributed binding of the copolymer with the tryptophan residues in the protein scaffold. The studies reveal that the copolymer holds potential for use in bioimaging and also as a protein sensor.

Introduction

Conjugated polymeric nanoparticles (CPNs) such as polyaniline (PANI)[1], polypyrrole (Ppy)[2], polythiophene (PTh)[3], and polycarbazole (PCz)[4] have lately received wide interest due to their high end applications in sensing, and imaging of biological moieties in the near infrared (NIR) region[5]. As compared to conventional dyes and inorganic quantum dots, CPNs reveal attractive optical properties such as high quantum yield, symmetrical emission spectra, broad-band excitation and polychromism due to confinement of their electronic states[6]. Morphologically induced polychromism has been investigated for poly (p-phenylenevinylene), poly(p-phenylene) and polythiophene family which has shown to influence their performance in bioimaging, LEDs, solar cells etc[7-9]. This phenomena is controlled by the polymer chain conformation, electronic structure, and polymerization conditions. Hence, tailoring of their structures is done to improve their processibility and fluorescent characteristics. One of the easiest methods adopted to improve their chemical properties is copolymerization with other monomers[10-12]. Functionalization via copolymerization allows for the introduction of various functional groups linked to the polymer backbone, which can alter the functionality of the polymeric materials[13-15]. The energy levels and bandgaps of the polymers can be effectively tuned to optimize their fluorescene behaviour by the selection of appropriate monomers. There are several reports on the copolymerization of aniline, thiophene, carbazole and their derivatives[16-18]. Poly(o-phenylenediamine) (POPD) has recently attracted attention because it has been reported to be a highly aromatic polymer containing 2,3-diaminophenazine units that

show high thermal stability[19-20]. *Sun et al*[21]. reported the synthesis of poly (o-phenylenediamine), poly(p-phenylenediamine) and poly (m-phenylenediamine) (PmPD) which were applied in the fluorescence detection of nucleic acid. Electrochemical synthesis has been widely reported for copolymerization of o-phenylenediamine with aniline[22], o-aminophenol[23], o-anisidine[24], o-toluidine[25], m-toluidine[26] and 1-amino 9,10-anthraquinone[27]. Scant work has been reported on the copolymerization of 1-naphthylamine with aniline and its derivaties[28] while no work has been reported on the copolymerization of 1-naphthylamine with o-phenylenediamine and o-anisidine via microwave synthesis. Till date, the nano synthesis of conjugated polymers has been reported using electropolymerization technique, template synthesis, seeding polymerization, interfacial polymerization, radiolytic synthesis, rapid mixing reaction, sonochemical synthesis, electrospinning, ferric chloride oxidation, template-free method which are detrimental to the environment due to the utilization of hazardous solvents and formation of toxic byproducts[29-31].

Microwave offers scope of very fast polymerisation and copolymerisation in presence of green solvents and in several cases also in its absence[31]. With the aim to achieve improved water solubility, controlled morphology as well as high quantum yield, the present work reports the synthesis of poly(o-phenylenediamine) (POPD), poly(1-naphthylamine) (PNA), poly(anisidine) (PAnis) and their mutual copolymers via microwave-assisted technique. The incorporation of electron-withdrawing/donating groups into the polymer main chain via copolymerization can control the electron/ hole-injecting/transporting capabilities of the resulting copolymers. It can also raise/reduce the HUMO/LUMO levels and can therefore help in achieving emission in the desired fluorescent range. The purpose of this study was also to utilize different functional monomers to investigate the probability of controlling the fluorescent characterisitcs of conjugated copolymers by choosing the appropiate functional monomer. We have therefore, chosen three monomers for polymerization as well as their copolymerization to study the influence of diamino group (o-phenylenediamine), methoxy group (o-anisidine) and a fused benzene ring (1-naphthylamine) on the copolymer structure and fluorescence efficiency.

Fluoresence quenching has been widely observed and investigated as a fundamental problem and in unravelling the structural dynamics of biological processes. Several biologically active molecules were found to quench the fluorescence of transport proteins through numerous forms of reactions, energy transfer, ground state complex formation, excited state reactions, molecular rearrangement and collisional quenching. Because of profound biological significance, quenching of bovine serum albumin's (BSA) fluorescence with drug molecules[32], inorganic moieties[33], gold and copper nanoparticles[34], TiO_2 semiconductor[35] and a host of composites[36] have been explored. However, fluorescence deactivation of bovine serum albumin (BSA) by conducting polymers have been scarcely investigated[37]. We, therefore, also aim to explore the fluorescence deactivation of BSA by POPD and POPD-co-PNA, the above synthesised and well charaterised water soluble homopolymer and copolymer to reveal the accessibility of these materials as quenchers to albumin's fluorophore groups, to elucidate mechanism of their interaction and also to get clues about the variation in binding phenomenon upon copolymerization.The study will expectedly open up opportunities for use of these polymers in in imaging of biologicl processes and in sensors.

Experimental

Materials

o-anisidine, o-phenylenediamine, 1-naphthylamine,ferric chloride ,methanol were procured from Sigma Aldrich, USA. Ferric chloride,N-methyl pyrolidone, acetonitrile,(Merck, India), were used without further purification.

Microwave-assisted synthesis of poly(1-naphthylamine), poly(o-anisidine)and poly(o-phenylenediamine)

1-naphthylamine (5g, 0.0349mol) was added to 100 ml Erlenmeyer flask containing water (25 ml). It was thoroughly dispersed by stirring. Ferric chloride (5g, 0.0308mol) dissoved in 10 ml water was added to the reaction mixture in 0.5 ml portions at two mintes intervals keeping the monomer : oxidant ratio 1:1.Afterwards the dispersion was irradiated by microwave for 15 min at 25^0C while bubbling nitrogen through it in a Ladd Research Laboratory microwave oven model LBP125-230 (220/230V), power source- 230 V ~50 Hz, energy output- 800 W, input power-1,200 W. The temperature of the oven throughout the synthesis was controlled by an in-built time and temperature controller. During micro wave processing, the colour changed from cream to dark purple which indicated the polymerization of 1-naphthylamine. The polymer obtained was then repeatedly washed with distilled water and methanol, dried in vacuum oven at 70˚C for 72 hours to ensure complete removal of adsorbed polymer, impurities, solvent and water. Similar procedure was adopted for the synthesis of poly (o-anisidine) and poly(o-phenylenediamine). The monomers taken were o-anisidine (5g, 0.0406mol) and o-phenylenediamine (5g, 0.046 mol) respectively. The polymers were designated as PNA, PAnis and POPD. Percent yield: PNA:76%, POPD:80%,PAnis:75%.

Synthesis of copolymers

1-napthylamine (NA) (8.949g, 0.25 mol) and o-anisidine (Anis) (7.048ml, 0.25 mol) were added to 100 ml Erlenmeyer flask containing water (25 ml). Ferric chloride (5g, 0.0308mol) dissoved in 10 ml water was added to the reaction mixture in 0.5 ml portions at two mintes intervals giving black colored dispersion. The reaction mixture was then subjected to microwave irradiation for 15 min at 25°C with continuous bubbling of nitrogen. Similar procedure was adopted for the synthesis of copolymers of o-phenylenediamine (OPD) (6.757g, 0.25mol) and o-anisidine (7.048 ml, 0.25mol) and o-phenylenediamine (6.757g,0.25mol) and 1-napthylamine (8.949g, 0.25 mol).The synthesized copolymer was then taken out and washed several times with distilled water and methanol

on a Buchner funnel. The removal of iron was ensured by testing the filtrate with potassium ferrocyanide. The obtained copolymers were then dried in vacuum oven for 72 hours at 70^0C to ensure complete removal of water and impurities. The synthesized copolymers were designated as : PAnis-co- PNA, POPD-co-PNA and POPD-co-PAnis.

Characterization

Intrinsic viscosites were determined by dissolving the polymers and copolymers (0.1wt%-1wt%) in NMP and measuring their viscosity at 25°C using Ubbehlode viscometer. Gel Permeation Chromatography was performed using Shimadzu Gel Permeation Chromatograph (GPC) equipped with refractive index and UV-Visible detector. 0.03% solution of copolymers were prepared in requisite amount of NMP containing 0.1% LiCl and a sample volume of 20 µL was injected into the column (Jordi-gel DVB mixed bed, 250 mm×10 mm) at 80 °C with a mobile phase flow rate of 1 mL/min at a column pressure of 5–6 MPa. The UV-Visible detector was set to a wavelength of 550, 560, and 450 nm respectively for copolymers POPD-co-PNA, POPD-co-PAnis, and PNA-co-PAnis. FT-IR spectra homopolymers and copolymers were taken in KBr pellets on FT-IR spectrophotometer model Shimadzu IRA Affinity-1. The integrated absorption coefficient, $\int \overline{adv}$, of NH absorption peak was determined using the IRA Affinity-1 software through Gaussian Lorentzian curve fittings as shown in Table.1. UV-visible spectra were taken on UV-visible spectrophotometer model Shimadzu UV-1800 using NMP as solvent. In precision analytical determinations integrated absorption coefficient is used in place of absorption coefficient at the maximum wavelength, λ_{max}. $\int adv$ was obtained from the area under the transition peak when the spectra was plotted as absorption coefficient vs. wave number. The area under the peak was obtained using Origin 6.1 which was standardized to Gaussian–Lorentzian shape. X-ray diffraction patterns of the nanocomposites were recorded on Philips PW 3710 powder diffractometer (Nickel filtered copper Kα radiation). Transmission electron micrographs (TEM) were taken on Morgagni 268-D TEM, FEI, USA. The samples were prepared by placing a dispersion of the sample on carbon-coated copper grid, subsequently drying in air before transferring it to the microscope, operated at an accelerated voltage of 120 kV.

Fluorescence spectroscopic studies were performed on fluorescencespectrophotometer Varian Cary Eclipse by preparing solutions of the polymers and copolymers in NMP. The quantum yield ϕ was calculated using the following equation and taking anthracene as reference material[38].

$$\phi_{sample} = \phi_{st}\left(\frac{I_{sample}}{I_{st}}\right)\left(\frac{\eta^2_{sample}}{\eta^2_{st}}\right)\left(\frac{A_{st}}{A_{sample}}\right)$$

Where n_{sample} and n_{st} are the refractive indices of sample and standard taken as reference (Rhodamine B), A_{sample} and A_{st} are the optical absorbance values of sample and reference of extremely dilute solution at the excitation maximum, I_{sample} and I_{st} are the emission intensity maximum of sample and standard taken as reference and Φ_{sample} and Φ_{st} are the quantum yield of sample and reference. Fluorescence images were obtained with a 100 X objective at room temperature using a Laser Confocal Microscope with Fluorescence Correlation Spectroscopy (FCS) - *Olympus FluoView™ FV1000* equipped with He-Ne laser and oil immersion objective. λ_{max} for laser excitation was 410 nm. The nanocomposites were placed on a glass slide covered with a cover slip.

Results and discussion

Intrinsic Viscosity and molarity

The homopolymers PAnis, PNA, and POPD showed intrinsic viscosities 0.66. 0.43 and 0.36 dLg^{-1} respectively, Table 1. Among the homopolymers, PAnis with highest intrinsic viscosity seemed to have more expanded chain structure because of the easy random orientation of its molecules. It appeared that POPD with lowest intrinsic viscosity had compact structure.This is also revealed by TEM in a later section. The copolymers POPD-co-PNA, POPD-co-PAnis, and PNA-co-PAnis revealed intrinsic viscosities equal to 0.53, 0.25, and 0.24 respectively having $\overline{Mw}$ values 8600, 6700 and 6400 respectively(given as supplementary information). These results showed that homopolymers had higher intrinsic viscosity than the copolymers, except POPD-co-PNA, which indicated that the above homopolymers had apparently larger monomer chains than the copolymers. It was also revealed that POPD and PNA, and POPD and PAnis monomer pairs had more compatibility for copolymerization than PNA and PAnis. *Li et al.*[39] have also reported the anumber average molar mass, Mw, of copolymer poly(ethylaniline-co-anisidine) in the range of 4370-7920 Da, having intrinsic viscosity in the range of 0.18-0.41dLg^{-1}.

Table 1 Polymerization reaction conditions of homopolymers and copolymers

Polymer/ copolymer	Monomer (mol)	Oxidant (mol) (ferric chloride)	Polymerization time (under microwave)	Polymerization temperature (under microwave)	yield (%)	Intrinsic Viscosity in NMP	$\overline{Mw}$ (GPC)	$\overline{Mn}$ (GPC)
PNA	0.034	0.030	15 min	20^0C	76	0.66	--	--
POPD	0406	0.039	15 min	20^0C	80	0.43	7500	5597
PAnis	0.040	0.036	15 min	20^0C	75	0.36	--	--
POPD-co-PNA	0.025 /0.025	0.030	15 min	20^0C	64	0.53	8600	6143
POPD-co-PAnis	0.025 /0.025	0.030	15 min	20^0C	60	0.25	6700	4589
PAnis-co-PNA	0.025 /0.025	0.030	15 min	20^0C	54	0.24	6400	4155

Confimation of homopolymerzation and copolymerization

On the basis of peak shift, intensities and comparing with the ^{1}H-NMR spectra of pure POPD,PNA, and PAnis, the peaks of ^{1}H-NMR spectra of copolymers were attributed to various specific protons (given as supplementary information). The POPD-co-PNA spectrum, revealed peak at 3.4 ppm attributed to free H_2O /DMSO. The peaks at 5.7 ppm and 6.3 ppm were attributed to –NH protons of PNA and POPD respectively. The peaks between 6.6 and 8.5 ppm were correlated to aromatic ring protons of PNA and POPD. The ^{1}H-NMR spectra of copolymer PNA-co-PAnis, yielded peaks at 3.4 ppm due to free H_2O/DMSO[40] .The peaks at 5.72 and 6.72 ppm arose from –NH

protons of PNA and PAnis respectively. Other peaks between 7.4 ppm to 9.0 ppm were correlated to aromatic ring protons of PNA and PAnis. The ^{1}H- NMR spectrum of copolymer POPD-co-PAnis, gave peak at 3.4 ppm attributed to free H_2O/DMSO[40] while the peaks at 7.01 ppm and 7.15 ppm arose from –NH protons of PAnis and POPD. The peaks between 7.3 ppm and 8.1 ppm were correlated to aromatic ring protons of POPD and PAnis. The ^{1}H-NMR spectra somehow did not reveal -OCH_3 protons in any of the copolymers that was reported to appear at 3.8 ppm[40] or, it was so small it could not be distinctly noticed. The peak at 3.4 ppm was observed in all the three copolymers and therefore could not be attributed to -OCH_3 proton. Moreover it matched more to free H_2O[40]. It was easier to find out the molar ratio of the components of the copolymer if either of them had a distinguishable functional group like -CH_3, -OCH_3,and such others. Since in the present case -OCH_3 protons were somehow not observed in the NMR spectra, the –NH protons of these components to find out molar ratio of the components in the copolymer chains.The molar ratio can roughly be calculated by comparing the integrated areas of –NH protons of each component were determined. Since per –NH proton there are 6 protons in naphthylamine (NA) monomer unit , 3 protons in anisidine (Anis) monomer unit, and 1.3 protons in o-phenylenediamine (OPD) monomer unit in the respective copolymer chains,The molar ratio of components in copolymer POPD-co-PNA, POPD/PNA = (-NH proton area of POPD)/1.3 ÷ (-NH proton area of PNA)/6 = (1.32/1.3 ÷ 1.0/6) = 86/14.. Molar ratio of components in copolymer PNA-co-PAnis, PAnis /PNA = (-NH proton area due to PNA)/6 ÷ (-NH proton area due to PAnis)/3 = (2.0/6 ÷ 2.55/3) = 28/72. Molar ratio of components in copolymer POPD-co-PAnis, POPD/ PAnis = (- NH proton area of POPD)/1.3 ÷ (-NH proton area of PAnis)/3 = (4.280/1.3 ÷2.4/3) = 80/20. The feed molar ratio of monomer components in each case of copolymer was 50/50. But NMR spectra revealed molar ratio of the monomers in copolymer chains much different from the above value. This happened because of different rate of growth of each monomer in the copolymer chain. In case of POPD-co-PNA, OPD monomer grew almost six times faster than NA monomers, hence more number of OPD units were formed in the copolymer than NA units. In the copolymer POPD-co-PAnis, OPD monomer grew four imes faster than Anis monomer. The anisidine monomer revealed more than two times faster growth rate than NA monomer in copolymer PAnis-co-PNA .It could be concluded that in copolymer formation OPD, grew fastest followed by Anis monomer and then NA monomer. These results also revealed random copolymerisation of participating monomers, Scheme 1.

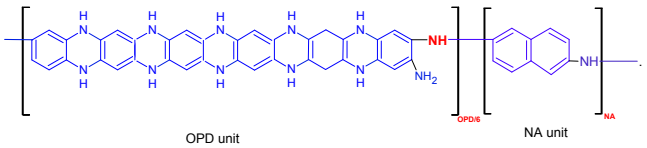

(a)

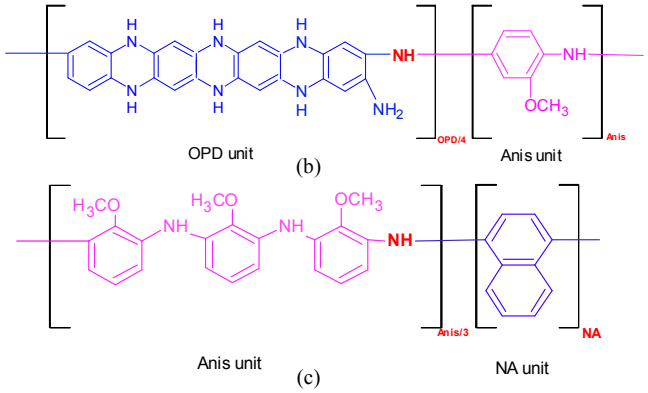

Scheme 1 Chemical structures of (a) POPD-co-PNA, (b) POPD-co-PAnis, (c) PNA-co-PAnis

Table 2 FTIR spectral data of pure polymers and copolymers

Sample	Vibrations of characteristic Bands/group	Peak Position (cm^{-1})/ Absorbance (Area cm^{-2} $\int adv$)
PNA	N-H stretching	3445-3070/1.1 **(175)**
	Imine stretching	1632/1.1 **(235)**
	C-C stretching (quinonoid)	1512/1.0 **(27)**
	C-C stretching (benzenoid)	1390/0.96 **(107)**
	C-N stretching (quinonoid)	1313/0.96
	C-N stretching (benzenoid)	1259/0.92
	C–H stretching (bending) of substituted benzene (1-4 coupling)	765/0.78
POPD	N-H stretching	3414 3230/2.01**(2173**
	Imine stretching	1635/1.4 **(83)**
	C–C stretching (quinonoid)	1529/ 1.76 **(256)**
	C–C stretching (benzenoid)	1475/1.27 **(36)**
	Phenazine skeleton	972-731/0.87
PAnis	N-H stretching	3448-3014/.49 **(907)**
	Imine stretching	1620/1.17 **(174)**
	C–C stretching (quinonoid)	1517/1.16 **(103)**
	C–C stretching (benzenoid)	1490/1.12 **(65)**
	Methoxy substituent	1250/1.00 **(104)**
	p-substituted benzene	842-621/0.65
POPD-co-PNA	N-H stretching	3446- 3313/1.73 **(753**
	Imine stretching	1608/1.45 **(151)**
	C–C stretching (quinonoid)	1597/1.41 **(344)**
	C–C stretching (benzenoid)	1473/1.36 **(263)**
PAnis -co-PNA	N-H stretching	3475-3014/1.59 **(276**
	Imine stretching	1682/1.25 **(314)**
	C–C stretching (quinonoid)	1508/1.19 **(236)**
	C–C stretching (benzenoid)	1400/1.06 **(158)**
	methoxy substituent	1260/0.995 **(88)**
	p-substituted benzene	773-721/0.64
POPD-co-PAnis	N-H stretching	3431/3032/1.28 **(285**
	Imine stretching	1690/1.25 **(310)**
	C–C stretching (quinonoid)	1597/1.15 **(262)**
	C–C stretching (benzenoid)	1473/1.15 **(223)**
	methoxy substituent	1261/0.999 **(65)**
	p-substituted benzene	896-750/0.73

The FT-IR spectrum data of pure PNA, Table 2, revealed an N-H stretching vibration peak spanning from 3445-3070 cm^{-1} for secondary amine with $\int adv$ value of 175 . The peak at 1632 cm^{-1} was assigned to the imine stretching mode while peaks at 1512 cm^{-1} and 1390 cm^{-1} were correlated to the ring puckering of the quinoid diimine and the benzenoid diamine units respectively. Other absorption peaks are the weak C–N stretching vibration at 1313 cm^{-1} due to the Q-B units and the 1259 cm^{-1} peak due to C–N stretching in B units. The peak at 765 cm^{-1} is produced by C–H out of plane bending. The peaks between 700 and 900 cm^{-1} usually occur due to C-H deformation mode and have been used to establish the position of coupling between two NA units. The coupling of 1,4 and 1,5 types are most favourable while 1,7 type is also observed[41] .The peak at 765cm^{-1} was consistent with the 1,4 coupling with two and 4 vicinal hydrogen on the two aromatic rings of 1-naphthylamine. The presence of the above peaks confirmed the polymerization of PNA[41].The peak area of benzenoid unit was found to be larger than the quinonoid quinonoid suggesting the formation of more benzenoid units. The ratio of the area of B/Q peaks was found to be 3.96. FTIR data of POPD , showed NH stretching vibration peak spanning from 3414-3230 cm^{-1}. The $\int adv$ of the NH in this case is observed to be 2173 which was highest among all polymers and copolymers. This can be attributed to the higher number of amino group in this polymer. The peak at 1635 cm^{-1} was assigned to the imine stretching while the peaks at 1529 cm^{-1}, 1475 cm^{-1} appeared due stretching vibrations of benzenoid and quinonoid units respectively. In this case, the area of quinonoid region appeared to be higher than the benzenoid region and the B/Q ratio was observed to be 0.14. The bands at 972-731 cm^{-1} were the characteristic of C–H out-of plane bending vibrations present on –benzene nuclei in the phenazine skeleton. The presence of the above peaks confirmed the polymerization of POPD containing more quinonoid units. PAnis, shows a broad band between 3448-3014 cm^{-1} due to the characteristic N-H stretching vibration. The $\int adv$ value for the NH region was noticed to be 907. In this polymer also, the quinonoid peak area was higher than the benzenoid peak area and the B/Q ratio was found to be 0.63. The band at 842-621 cm^{-1} corresponded to the C-H bending vibrations present in the p-substituted benzene ring. The FTIR data of POPD-co-PNA, showed NH stretching vibration band spanning between 3466-3313 cm^{-1} with the $\int adv$ value of 753. The area of the NH region was higher than pure PNA and lower than pure POPD suggesting random copolymerization of the two monomers. The imine peak is found to shift to 1608 cm^{-1} and the peak area is observed to be 151. The $\int adv$ values of quinonoid and benzenoid regions were observed to be 344 and 263 indicating the presence of higher number of quinonoid groups than bezenoids, while the B/Q ratio was also found to be 0.76. The band at 796-617 cm^{-1} corresponded to the C-H bending vibrations of the p-substituted benzene ring[28-29].

This observation confirmed the expected head-to-tail coupling copolymerization of 1-naphthylamine with o-phenylenediamine at the C-4 position[25-26]. Likewise, the copolymer of PAnis-co-PNA, showed a broad NH stretching vibration region between 3475-3014 cm^{-1} with an $\int adv$ value of 276. The area appears to be quite reduced as compared to the previous copolymer and its homopolymer as well. The imine strecthing mode also shifted to higher values which can be attribtued to the steric hinderance created by the methoxy substituent of PAnis in copolymerization. The B/Q ratio was observed to be 0.66 and the area of the quinonoid groups appears a little higher than the benzenoid groups. Incase of POPD-co-PAnis, $\int adv$ value for the NH region was higher then the previous copolymer while the area of benzenoid and quinonoid units was observed to be comparable. B/Q ratio was found to be 0.85 suggesting equal number of benzenonoid and quinonoid units. Deformation mode of imine stretching showed bonding between aromatic moieties . Imine deformation mode in PNA, POPD, and PANIS was respectively observed at 1632 cm^{-1} ,1635 cm^{-1}, and 1620 cm^{-1}. A large shift in imine deformation mode in case of these copolymers was observed. The above for POPD-co-PNA, POPD-co-PAnis, and PAnis-co-PNA are found at 1608 cm^{-1}, 1682 cm^{-1} and 1690 cm-^{1}. Such large change in imine deformation mode peak values indicated copolymerization of interacting monomers. The presence of both bezenoid and quinonoid rings in both the homopolymers and copolymers revealed their semiconducting state.

Confirmation of polaronic states of homopolymers and copolymers

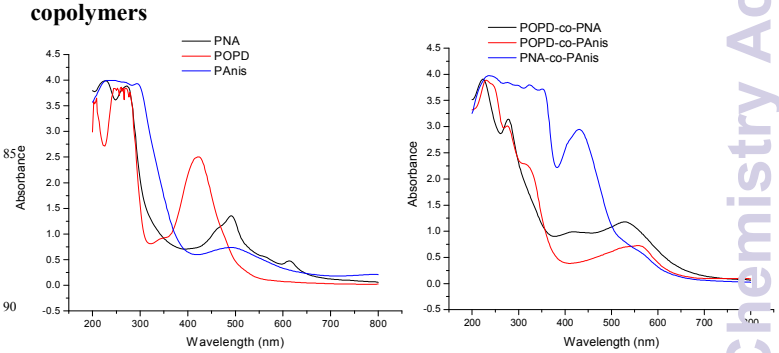

Fig.1 UV-visible spectra of PNA, POPD, PAnis and its copolymers

The UV –visible spectrum of PNA in NMP, Fig.1 (a), showed peaks at 220 nm, 280 nm in the UV range and at 500 nm and 610 nm in the visible range. The peak in the UV range was assigned to π-π^* transitions. The peak at 500 nm was correlated to the excitonic transitions while the one at 600 nm in the visible region was assigned to the polaronic transitions[41]. The later peak corresponded to conducting state. The UV–visible spectrum of POPD in NMP, Fig.1 (a), revealed two major peaks, in the UV region, one at 200 nm, the other at 250 nm and another peak at 452 nm. The band at 452 nm was due to exciton formation indicating nearly semiconducting state and the transition was associated with the benzenoid to quinonoid transition. Similarly, the UV-visible spectrum of PAnis, Fig.1(a), showed a broad peak at 250 nm in the UV range while the peak at 500 nm corresponded to excitonic transitions.

Incase of the copolymer of POPD-co-PNA, Fig.1(b), the spectrum showed 2 peaks in the UV range at 225 and 275 nm respectively and one peak in the visible range at 530 nm

respectively. As these peaks were not present in the homopolymers, they confirmed the copolymerization via reorganization of the monomer units. Similarly for POPD-co-PAnis, Fig. 2(b), we observed three peaks in the UV range at 250 nm, 260 nm and 310 nm respectively and only one peak was observed in the visible range at 550 nm not found in the two monomers which also veified copolymerisation between the same monomers. In the case of PNA-co-PAnis, Fig.2(b), the excitonic peak was observed at 430 nm and showed a dramatic blue shift. In this case steric hindrance due to methoxy group and its electron withdrawing effect caused a large blue shift. This established copolymerisation between o-anisidine and 1-naphthylamine.

Crystallinity and morphology of homopolymers and copolymers

The peak analysis of these diffractograms was carried out using Origin 6.1 software. The inter-chain separation length (R) corresponding to the highest intense crystalline peak was determined from the relation Klug and Alexander[42]:

$$R = \frac{5\lambda}{8\sin\theta}$$

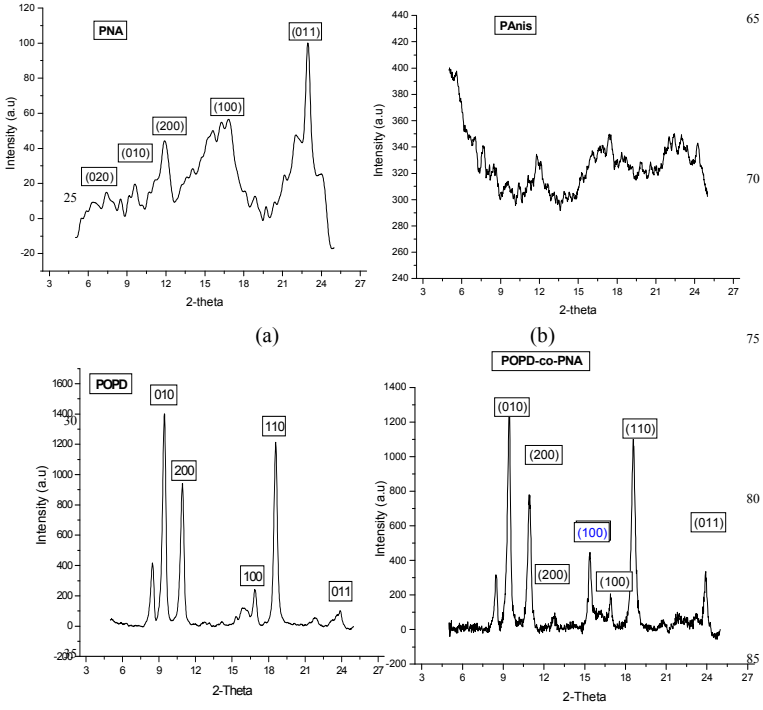

(a) (b) (c) (d)

The phase in which the polymer chains are parallel and ordered in close packed array is the crystallites region, whilst the phase where the chains are not ordered and do not have parallel alignment is the amorphous region. The ordered arrangement of polymer chains in the crystalline phase may be of different types depending on the nature of the polymer, and can be detected from X-ray diffraction study.

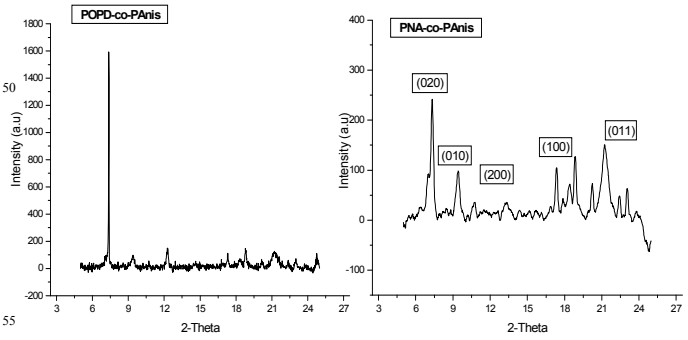

(e) (f)

Fig.2 XRD diffractograms of pseudo orthorhombic (a) PNA (b) PAnis (c) POPD (d) POPD-co-PNA (e) POPD-co-PAnis (f) PNA-co-PAnis

Peaks were observed for PNA, Fig.2(a), at 7.4 Å, 9.6 Å, 11.9 Å,16.8 Å and 22.9 Å correspomding to (020), (010), (200), (100) and (011) planes, indicating that the majority of PNA chains were ordered along these three crystal planes of a pseudo orthrhombic lattice as reported by other authors[43-44]. Close agreement was observed between the observed and calculated values of an orthorhombic cell having $\alpha=\beta=\gamma=90^{\circ}$ and a = 5.2007 Å, b = 9.7743 Å,c = 4.2711 Å). The sharpness (width) of the peaks revealed the degree of orientation of the polymer chains in that particular crystal plane, and the intensity (peak height) represents the population of crystallites in that plane. It was found that for PNA ,Fig.2(a), the sharpness as well as the intensty of (011) plane was maximum. The interchain distance was calculated to be 2.46 Å. The higher degree of ordering of the polymer chains was attributed to interchain hydrogen bonding between adjacent polymer chains. The X-ray diffractogram of PAnis, Fig.2(b), showed the existence of several broad peaks which indicated that crystallites in these planes were oriented in different directions. This occured presumably due the steric hinderance of the methoxy substituent present in PAnis. For POPD, Fig.2(c), the structure appers to be well organized. Peaks were observed at 9.45 Å , 10.97 Å, 16.9 Å and 18.6 Å and 23.5 Å corresponding to (010) , (200), (100), (110) and (011) planes. The sharpness of the (010) plane is observed to be highest and the interchain distance was calculated to be 5.86 Å.This indicated that the polymer chains in POPD were more regularly ordered but not well compacted because of inter-chain H-bonding through amino groups which remain laterally stretched and did not allow the polymer chains to come closer. Most of the peaks appeared to be sharp in the copolymer indicating highly ordered orientation of the copolymer chains. For POPD-co-PNA, additional planes of PNA were clearly observed in the copolymer while the peaks pertaining to POPD appeared to be more sharp as compared to pure homopolymer. Likewise for POPD-co-PAnis, Fig.2 (e), the peak at 7.3 Å appeared to be sharp and well formed and the interchain separation was calculated as 7.5 Å which was matching with the preceding copolymer having POPD with laterlly oriented amino group causing loose packing. Incase of PAnis-co- PNA, Fig. 2(f), semicrystallinity was observed as inter chain hydrogen bonding was least expected in this copolymer and the chains have lesser opportunity to organise in ordered manner. The interchain

separation of this copolymer revealed a loosely packed structure. TEM micrograph of pure PNA, Fig.3(a), revealed a petal like morphology and the the particles size were calculated to be 250 - 290nm. The dark sphere represented the nucleus which generated a controlled pattern of coral like leaves. This can also be correlated to the XRD of the said polymer which showed a partially ordered morphology of low interchain separation. The morphology of POPD, Fig.3(b), revealed aggregation of small rods of 200 nm in diameter and 400 nm in length . The rods were formed by folding of the polymer chains and their lateral growth. XRD also corroborated this morphology which indicated distorted orthorhombic lattice. The TEM of PAnis, Fig.3(c), revealed very small spherical particles joining each other and forming fine fibrils, the latter forming bundles of aggregated fibers. The XRD also showed an amorphous strucutre which matched well with the TEM. The morphology of POPD-co-PNA,Fig.3(d), showed the formation of spherical particles ranging between 270 nm-300 nm. The spheres appeared to be well form and of similar size. It can be concluded that the spherical morphology oriningated by spherical wrapping up of the copolymer chains.

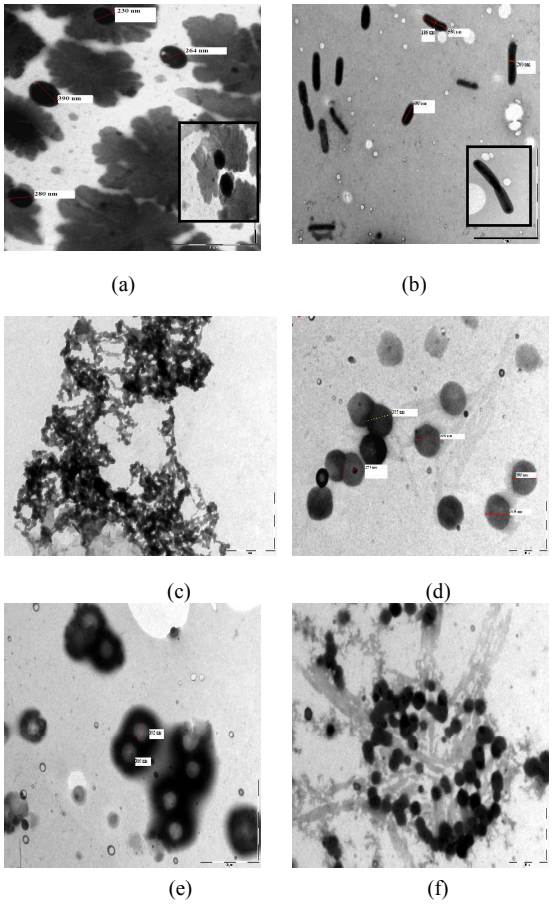

(a) (b) (c) (d) (e) (f)

Fig.3 TEM of (a) PNA, (b) POPD (c) PAnis, (d) POPD-co-PNA, (e) PNA-co-PAnis, (f) POPD-co-PAnis

The TEM of PAnis-co- PNA, Fig.3(e), revealed a distorted spherical morphology where the spheres appeared to undergo fusion and were also elongated. The spheres showed hollow core as if folding of chain occured leaving a circular space. XRD of the same also revealed a semicrystalline morphology which matched well with the TEM. However, POPD-co-PAnis, Fig.3(f), revealed morphology of small spheres which fused with each other preferably length wise. It can be concluded that microwave produced structures of controlled morphology. Incase of copolymerization, the morphology was observed to be entirely different from the homopolymers which clearly confirmed copolymerisation of monomer pairs and that the copolymer units reorganized themselves and produced entirely different morphology from the homopolymers. Thus, by polymerization under microwave irradiation and by choosing the right combination of monomers for copolymerization, one can obtain self-assembled structures of desired morphology.

Fluorescence charactertisics

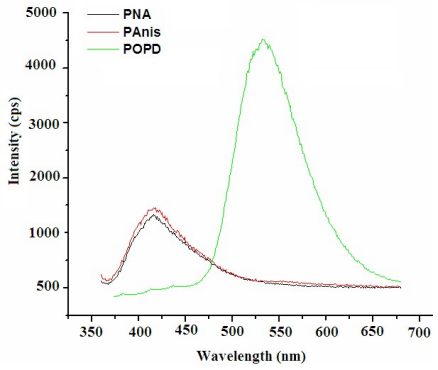

(a)

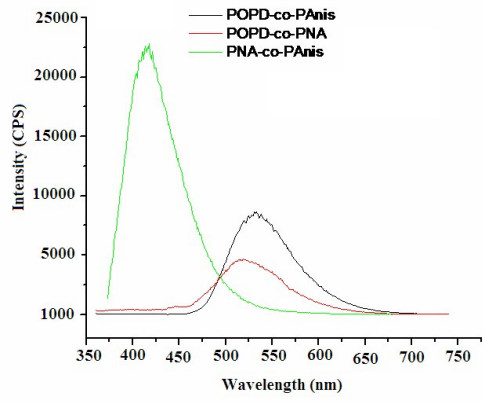

(b)

Fig.4 Fluorescence emission spectra (excitation wavelength =330 nm) of (a) homopolymers (b) copolymers

The emission spectrum of pure PNA and PAnis, Fig.4 (a), revealed an emission peak at 416 nm upon excitation at 330 nm. Both the homopolymers showed peaks in the UV region at 300 nm for $So \rightarrow S_1$ transition. However the emission spectrum of POPD, Fig. 4(a), revealed an emission peak at 540 nm corresponding to transition of $So \rightarrow S_1$ peak at ~ 425 nm.

The spectrum of POPD-co-PNA, Fig.4 (b), exhibited a relatively low intensity peak of about 3000 cps at 531 nm. This showed that the number of decaying excited state copolymer molecules were reduced, or, HOMO and LUMO were

not symmetrically disposed. Liksewise, POPD-co-PAnis also ,Fig.4(b), revealed a broad peak at 521 nm of intensity about 7500 cps which was higher than both the contributing hompolymers. In this case, HOMO and LUMO appeared to be symmetrically disposed. From peak positions of POPD-co-PNA and POPD-co-PAnis, it can be inferred that these copolymers were dominated by POPD comonomers as was also revealed by ^{1}H NMR. PNA-co-PAnis showed a sharp and intense emission peak at 418 nm. The UV-vis peak of PAnis-co-PNA was observed at 450 nm revealing a noticeable blue shift comparing with the the emission peak of 418 nm of the copolymer. This difference arose because of the use of excitation pulse of 330 nm to get the fluorescence spectrum, othewise the absorption and emission spectra were almost mirror image of each other. It means that the number of excited molecules and enegy of transition for $S_o \rightarrow S_1$ is the same as for fluorescence energy $S_1 \rightarrow S_o$ in this case. Interestingly copolymer peak position of PAnis-co- PNA was almost similar to its homopolymers and the latter had almost equal emission intensities,1400 cps, but that of the copolymer was far much enhanced, equal to 22000 cps. Enhancment in fluorescence intensity appeared to occur through the non radiative enegy transfer by each monomer to the emission energy of its co-monomer, i.e, Foster energy transfer takes place. Copolymerization can therefore be used to control the fluorescence of the semiconducting polymers and can also be used to tune in the emission either in the UV region or in the visible region through the selection of appropriate combination of the monomers.The values of Φ for PNA, PAnis and POPD were respectively found to be 0.04, 0.04, 0.07 while for the copolymers POPD-co-PNA, POPD-co-PAnis and PAnis-co-PNA, they were observed to be and 0.15, 0.08 and 0.06 respectively,Table 3.

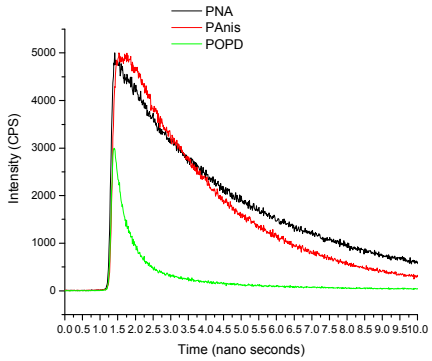

(a)

The fluorescence decay time τ, determined in solvent NMP **was** inversely proportional to the Φ, i.e., lower the decay time higher the quantum yield. The decay time was determined from the curves by reading off the time at 36.8% fluorescence intensity[45].

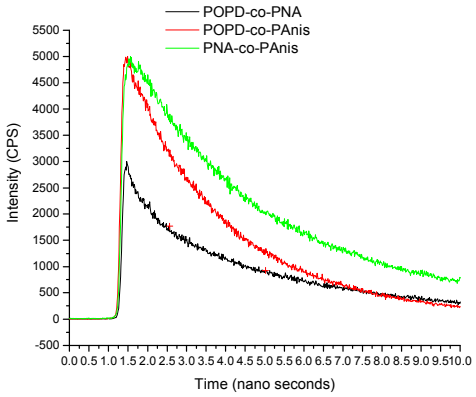

(b)

Fig.5 Fluorescence decay profiles of (a) homopolymers (b) copolymers

Table 3 Integrated area and Relative quantum yield values

Sample	Integrated Area 550 nm (cm^{-1})	Optical density 416/ 550 nm	Quantum yield
Rhodamine B	80000000	0.05	0.5
PNA	14676544	0.13	0.04
PAnis	16341178	0.14	0.04
POPD	29332623	0.13	0.07
POPD-co-PNA	59891339	0.14	0.15
POPD-co-PAnis	34643017	0.15	0.08
PAnis-co- PNA	25154200	0.13	0.06

The decay time for pure PNA, PAnis and POPD was observed to be 5.25 ns, 4.75 ns and 2.0 ns while for POPD-co-PNA, POPD-co-PAnis and PAnis-co- PNA it was observed to be 4.25 ns, 4.5 ns and 5.5 ns repsectively, Fig.5 (a),(b).The experimental values of Φ and τ show inverse relationship as expected.

BSA quenching studies with POPD and POPD-co-PNA

BSA is a carrier protein which carries drug molecules to target tissues. BSA shows a wide range of physiological functions based on the binding, transport and distribution of drugs and other biologically active molecules. BSA has two tryptophan groups (Trp-134 and Trp-212) which fluoresce at 350 nm.

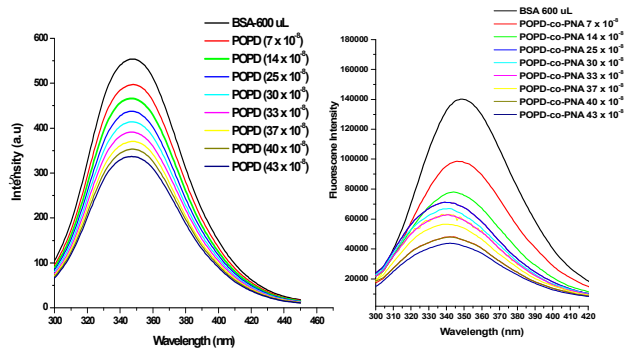

(a) (b)

Fig.6 Fluorescence spectra of quenching of BSA by (a) POPD (b) POPD-co-PNA

The latter tryptophan residue is buried in a hydrophobic sack lying near the surface of the albumin molecule in the second α-helix of the first domain[46]. The fluorescence of tryptophan residues can be quenched either through energy or electron transfer by drug and other reactive molecules. Quenching of BSA therefore implies conformational changes, transition inmicroenvironment, binding with drug and other biologically active molecules, denaturation and subunit association. As POPD and POPD-co-PNA were found to be soluble in water in the experimental limit, quenching of the fluorescence of bovine serum albumin by these conjugated polymers was explored. The quenching of the BSA by these polymers occured either through noncovalent interaction, electron or energy transfer.Since fluorescence intensity of these conducting polymers is not enhanced during quenching, possibility of energy transfer is minimal[46]. The quenching of BSA therefore occurs through either noncovalent interaction or by photo-induced electron transition. The quenching of the fluorescence emission mechanistically occurs either from static or dynamic interaction of the quencher with the fluorophore. In order to assess the quenching mechanism of BSA fluorescence, we monitored the emission of tryptophan residues in the protein solution at different concentrations of the quencher. It was observed that upon titration of BSA with POPD and POPD-co-PNA,Fig.6(a),(b), the fluorescence emission maxima of BSA was found to decrease. The quenching of POPD with BSA revealed notable shift in the peak intensity while a prominent blue shift (from 350 to 340 nm) is noticed incase of POPD-co-PNA due to the local interaction of the latter with BSA resulting in the loss of compact structure of hydrophobic sub-domains containing tryptophan[45]. This can be correlated to a variety of molecular interactions, such as, ground state complex formation, energy and electron transfer, and collisional quenching that can occur between POPD and POPD-co-PNA with BSA.

The fluorescence quenching is described by Stern–Volmer relation[47]:

$F_0/F = 1 + KSV[Q] = 1 + kq\tau_0[Q]$

where F_0 and F are the fluorescence intensities in the absence and presence of quencher, KSV is the Stern–Volmer constant related to the bimolecular quenching rate constant, k_q, $KSV = k_q\tau_0$, and τ_0 is the average lifetime of BSA evaluated as 10^{-8} s. For determining the quenching and binding constants, molar masses of POPD and POPD-co-PNA as determined by GPC ,Table 1.

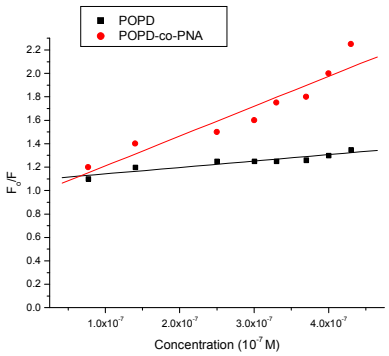

(a)

The quenching rate constant k_q obtained for POPD-co-PNA was 2.0 x10^{14} $LM^{-1}s^{-1}$ while for POPD it was observed to be 1.08 x 10^{14} $LM^{-1}s^{-1}$. K_{SV} for POPD-co-PNA and POPD was found to be 2.0 x 10^6 L M^{-1} and 1.08 x 10^6 L M^{-1}. The calculated quenching rate constant was far greater than the value obtained for biological macromolecules due to the collision mechanism (2.0 x 10^{10} LM^{-1} s^{-1})[49-51].

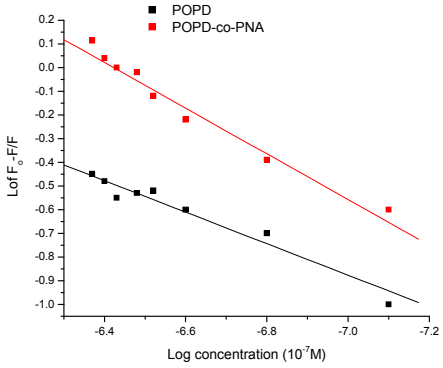

(b)

Fig.7 (a) Stern Volmer plot for of fluorescence quenching of BSA by POPD and POPD-co-PNA (b) plot of log F_o-F/F vs log concentration

This shows that the quenching of BSA by copolymer POPD-co-PNA and polymer POPD is static through the formation of an intermolecular complex, and is not initiated by dynamic collision. The binding constant and the number of binding sites were calculated using the equation[50-52]:

$$\log\frac{F_o - F}{F} = \log K_a + n\log[Q]$$

K_a, n and Q are the binding constant,the number of binding sites, and concentration of the quencher respectively. The K_a value for POPD was oserved to be 3.98 x 10^6 LM^{-1} while n was observed to be 0.7. For POPD-co-PNA, K_a value was found to be 1.26 x 10^7 L M^{-1}, and n was 0.96 which is higher than the values obtained by *Feng et al*[53]. They designed a biosensor based on bovine serum albumin (BSA) and poly-o-phenylenediamine (PoPD)/carbon-coated nickel (C-Ni) nanobiocomposite film

modified electrode to study the interaction of BSA with papaverine (PAP). The Ka and n values reported by them was, $K_a = 2.1\times10^4\ LM^{-1}$, n = 1. For Au nanoparticles, the ,binding constant K and the binding sites n were observed to be 1.97 x 10^2 LM^{-1} and 0.6 respectively[54].The excited tryptophan group of albumin gives out electron which is taken up by easily reducible conductive copolymer POPD and POPD-co-PNA that results, into forming a ground state intermolecular complex with BSA.

Confocal microscopy analysis

This technique gives a visual evidence of interaction of BSA with POPD as well as POPD-co-PNA. On excitation of POPD-BSA complex, POPD particles became visible but had low intensity and were less widely distributed ,Fig.8(a). This was correlated to their lesser interaction with BSA as was observed in the preceding section as well as their low life times. However on excitation of POPD-co-PNA-BSA complex, Fig.8(b), the copolymer particles appeared more bright because of thier relatively larger life times and were widely distributed due to the higher interaction with BSA as was noted from the quenching and binding rate constant which were higher than POPD.

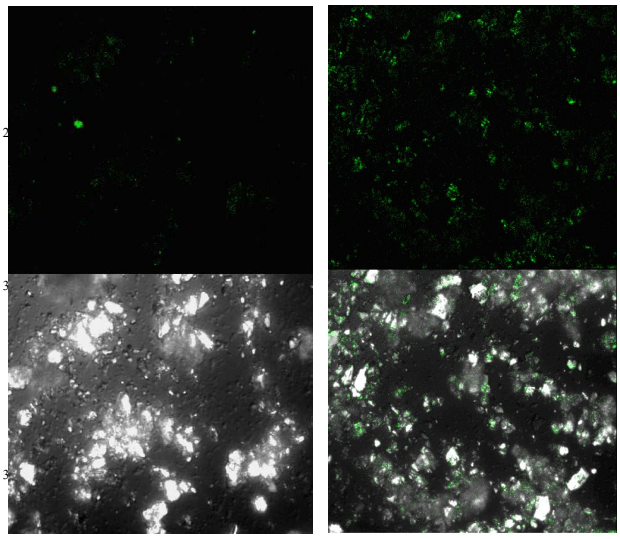

(a) (b)

Fig.8 Confocal images of (a) POPD quenched BSA (b) POPD-co-PNA quenched BSA

Conclusion

Microwave irradiation provides an easy and fast method for polymerization and copolymerization of conducting polymers. Pristine homopolymers and copolymers of PNA, POPD and PAnis were synthesized via microwave-assisted technique. FTIR spectra confirmed copolymerization while UV–visible spectra showed the influence of the monomer functionality on the polaronic transitions. Highly crystalline morphology was attained for POPD. Likewise POPD-co-PNA copolymer also revealed high crystallinity and controlled morphology of spheres of uniform size. The life time of POPD-co-PNA, a lesser water soluble copolymer, was found to be 4.25 ns and that of POPD 2.0 ns which matches with life time scale 1-10 ns of biological processes, they can hence be used in imaging of biological events. Confocal microscopy shows scintillating green copolymer particles widely spread on BSA scaffold. The studies of BSA quenching revealed that POPD-co-PNA bound much strongly with the former as compared with homopolymer POPD. The binding constant of POPD-co-PNA with BSA is comparable with other quenchers. The quenching occurs through photo induced electron transfer. It was spectroscopically confirmed that quenching of BSA followed the static mechanism. These results reveal that the POPD-co-PNA holds potential for application also as biosensor. Results show that copolymerization can also be used to tune in the emission either in the UV region or in the visible region through the selection of appropriate combination of functional monomers.

Acknowledgement

The corresponding author Dr Ufana Riaz wishes to acknowledge the Department of Science and technology (DST)-science and engineering research board DST-SERB, India vide sanction no. SB/S-1/PC-070-2013 for granting major research project.The author also wishes to acknowledge the SAIF Facility at All India Institue of medical Sciences, for providing the TEM analysis.

References

1. Z.Liu, B.Ye, M. Jin, H.Chen, H.Zhong, X.Wang, Z. Guo, *Nanoscale*, 2015,**7**, 6754-6761.
2. J. Li , J. Han, T. Xu , C. Guo, X. Bu , H. Zhang, L. Wang, H. Sun and B. Yang, *Langmuir*, 2013, **29 (23)**, 7102–7110.
3. J.M. Liu, J.T.Chen and X.P. Yan**,** *Anal. Chem.*, 2013, **85(6)**, 3238–3245
4. P.E. Danjoua, J.Lyskawaa, F. Delattrea, M.Becuwea, P. Woisela, S. Ruellana, S. Fourmentina, F.C.Dennina, *Sens.Actuat*. B*Chem*.**,** 2012, **171–172**, 1022–1028.
5. U.Riaz and S.M.Ashraf, Computational Optical Biomedical Spectroscopy and Imaging, CRC press, 2015 Edn, Pg 27-65.
6. G.Sonmez , H.Meng and F.Wudl **,***Chem. Mater.*, 2004, **16 (4),** 574–580.
7. A.Köhler, S.T.Hoffmann, H.Bässler, *J. Am. Chem., Soc.*, 2012, **134 (28)**, 11594–11601.
8. R.Liu, Y.Li,K.P.Seah,B.Liu,N.Tomczak, *Eur.Polym.J*., 2014, **50**, 46–53.
9. W. Bai ,C.Wu, X. Shang, L. Cai, J.Lin, *Euro Polym.J*., 2015,**70**, 221–231.
10. C. S. Fischer, C.Jenewein and S. Mecking**,** *Macromolecules*, 2015, **48(3),** 483–491.
11. S.W. Chang and M.Horie, *Chem. Commun.*, 2015, **51**, 9113-9116.
12. J. Xia, L. Huang, K.Peng and T.Pei, *RSC Adv.*, 2015(in Press).
13. G. M. Miyake and J.C.Theriot**,** *Macromolecules*, 2014, **47(23),** 8255–8261.
14. A.Bousquet , H.Awada, R.C.Hiorns, C.D.Lartigau, L.Billon, *Prog.Polym.Sci*., 2014,**39**, 1847–1877.
15. J.Terao, K.Homma, Y.Konoshima, R.Imoto, H. Masai, W.Matsuda,S.Seki,T.Fujihara, and Y. Tsuji, *Chem. Commun.*, 2014,**50**, 658-660.
16. U.J.Male, B.S.Singu, P.Srinivasan, *J.Appl.Polym.Sci.,* 2015,**132(37)**,42013.
17. R.B.Moghaddam, P.G.Pickup,*Electrochim. Acta,* 2013,**107**, 225–230.
18. J. H. Park, T.W. Koh, J. Chung, S. H. Park, M. Eo, Y. Do, S. Yoo and M. H. Lee, *Macromolecules*, 2013, **46 (3),** 674–682.
19. J. Stejskal, *Prog.Polym.Sci.*, 2015**, 41**,1–31.
20. Y.Zhu, B. Zhang, Z. Feng, D. S. Su, *Catalysis Today*, 2015,(In press).
21. Y.Zhang, L. Wang, J. Tian, H. Li, Y. Luo and X. Sun, *Langmuir*, 2011, **27(6),** 2170–2175.
22. H. Peng, C. Liang, A. Zhou, Y. Zhang, Q. Xie, S. Yao, *Anal.Chim.Acta*, 2000,**423**,221–228.

23. D. L. J. Broere, R. Plessius and J. I. Vlugt, *Chem. Soc. Rev.*, 2015,(In press).
24. X.G. Li, W. Duan, M.R. Huang and Y.L. Yang, *J. Polym. Sci Part A: Polym.Chem.,* 2001**,39**,3989–4000.
25. S. Bilal, R. Holze, *J Electroanal.Chem*., 2006, **592**, 1–13.
26. S. Bilal, R. Holze, *Electrochim. Acta.,* 2007, **52**,5346–5356.
27. L. A. Hernandezi, M. A. D.Valle, F. J. Armijo, F. R. Diazi, G. Louarn, *Electrochem*., 2013, **81**,954-960.
28. U. Riaz, R. Jahan, S. Ahmad and S. M. Ashraf, *J. Appl.Polym.Sci*., 2008,**108**, 2604–2610.
29. U. Riaz, S. Ahmad, S. M. Ashraf, *Nanoscale Res.Lett.,* 2008, **3**,45-48.
30. J. Pecher and S. Mecking , *Chem. Rev.*, 2010, **110(10)**, 6260–6279.
31. A. Kumar, B. Behera and S. S. Ray, *RSC Adv.*, 2015,**5**, 39474-39481.
32. Y. Yu, S. Y. New, J. Xie, X. Su and Y. N.Tan, *Chem.Commun.***,** 2014,**50**,13805-13808.
33. J.W. Liu , Y. Zhang, X.W. Chen and J.H. Wang*, ACS Appl. Mater. Interface.,* 2014, **6(13),**10196–10204.
34. N. Zhang, Y. Si , Z. Sun, L. Chen, R. Li, Y. Qiao and H. Wang, *Anal. Chem.*, 2014, **86 (23)**,11714–11721.
35. L. Z. Zhao, Y. S. Zhao, H. H. Teng, S. Y. Shi, B. X. Ren, *J. of Appl. Spec.*, 2014, **81**, 719-724.
36. A.Ghosh, V. Jeseentharani, M. A. Ganayee, R. G. Hemalatha, K**.** Chaudhari, C. Vijayan**,** and T. Pradeep, *Anal. Chem.*, 2014, **86 (22),** 10996–11001.
37. R. A. Khanbeigi, Z. Hashim, T. F. Abelha, S. Pitchford, H. Collins, M. Green and L. A. Dailey, *J. Mater. Chem. B***,** 2015,**3**, 2463-2471.
38. U. Riaz and S. M. Ashraf, *J. Phys. Chem. C*, 2012, **116**, 12366-12372.
39. X-G.Li, M.Huang, W.Feng, M.Zhu, Y.Chen, *Polymer*, 2004, **45**,101-115.
40. X-G Li, W.Duan, M-R. Huang,Y-L.Yang*, J.Polym.Sci.PartA, Polym.Chem.* 2001,**39**,3989-4000.
41. U.Riaz, S.Ahmad and S.M.Ashraf, *Des,Monom.Polym*. 2008,**11(2)**,201-214.
42. H.P. Klug and L.E. Alexander, *X-ray Diffraction Procedures*. Wiley-Interscience, New York, chap. 1974,12.
43. D.K.Ray,A.K.Himanshu,T.P.Sinha,*Ind.J.Pure.Appl.Phy*. 2007,**45**,692-699.
44. D.K.Ray,A.K.Himanshu,T.P.Sinha,*Ind.J.Pure.Appl.Phy*. 2005,43,787-793.
45. D.Jameson, Basic Fluorescence Principles II, *Weber Conference on Advanced Fluorescence Microscopy Techniques*, Buenos Aires, December 12-17, 2011.
46. D.Carter,J.X.Ho, *Adv.Protein.Chem*.,1994,**45**,153–203.
47. C.Banerjee, J.Kuchlyan, Debasis Banik, Niloy Kundu, A.Roy,S.Ghosh and N.Sarkar *Phys.Chem.Chem.Phys***.,**2014, **16**, 17272-17284.
48. A.Garai, S.Chatterjee and, A.K. Nandi, *Polym.Engg.Sci*.,2010 **50(3)**, 446-454.
49. Z.Tian, F.Zang, W.Luo, Z.Zhao, Y.Wang, X.Xu, C.Wang. *J.Photochem.Photobiol. B, Biol*., 2015,**142**,103-109.
50. A.Divsalar, Md.J. Bagheri, A. Saboury, H.M. Torshizi, M. Amani, *J. Phys. Chem. B.,* 2009,**113,**14035–14042.
51. A.Bhogale, N. Patel, P. Sarpotdar, J. Mariam, P.M. Dongre, A. Miotello, D.C.Kothari, *Colloids Surf., B*.,2013,**102**,257-262.
52. O.K. Abou-Zied, O.I.K. Al-Shihi, *J. Am. Chem. Soc*. 2008,**130**,10793–10801.
53. L-J.Feng, X-H.Zhang, D-M.Zhao, S-F.Wang,*Sens.Actuat.B, Chem*., 2011,**152**,88–93.
54. S.Singh, R.Kaur, J.Chahal, P.Devi, D.V.S.Jain, M.L.Singla *J.Lumin*. 2013,**141**, 53–59.

Graphical Abstract

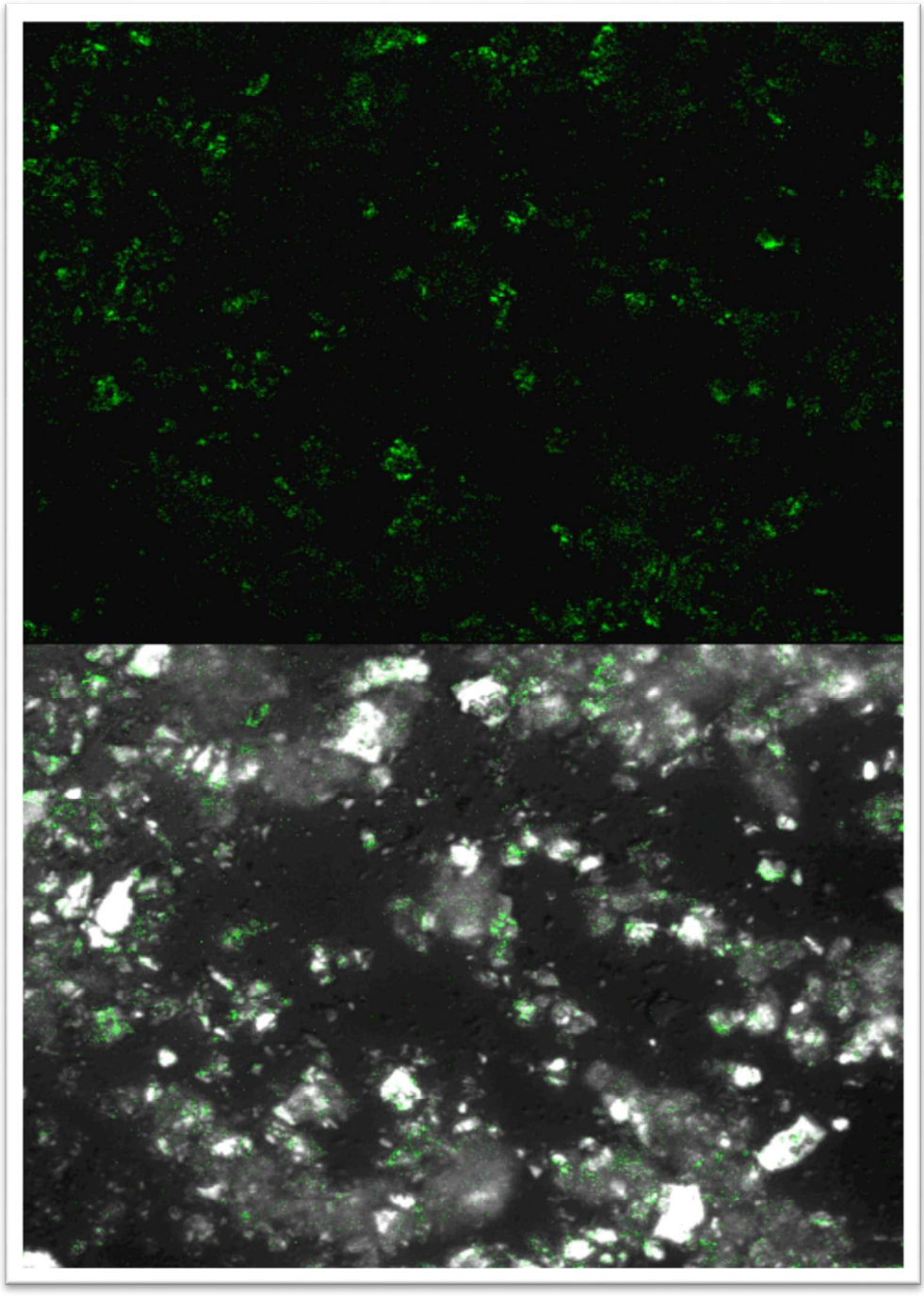

The copolymer POPD-co-PNA quenches BSA fluorescence revealing many of its photophysical characteristics including higher association constant and its scintillating presence on the later